

The Spring-Connected Rigid Block Model Based Automatic Synthesis of Planar Linkage Mechanisms: Numerical Issues and Remedies

Sang Jun Nam

Samsungtechwin R&D Center,
Seongnam-si,
Gyeonggi, 463-400, Korea

Gang-Won Jang

Faculty of Mechanical and
Aerospace Engineering,
Sejong University,
Seoul 143-747, Korea

Yoon Young Kim¹

Mem. ASME

WCU Multiscale Design Division,
School of Mechanical and
Aerospace Engineering,
Seoul National University,
Seoul 151-742, Korea
e-mail: yykim@snu.ac.kr

Because it is difficult to select in advance an appropriate linkage for converting an input motion to a desired output motion, a linkage synthesis method that does not require any baseline linkage would be preferred. To this end, an optimization-based linkage synthesis method that employs a spring-connected rigid block model has recently been suggested and applied for open-path problems. The objective of this study is to expand the method for the synthesis of more complex linkage mechanisms such as closed-loop linkages. Because the direct application of the method originally developed for open-path problems causes several numerical difficulties for closed-loop problems, an alternative optimization-based synthesis formulation is proposed in this investigation. The effectiveness of the suggested formulation is verified through several case studies including the synthesis of mechanisms generating closed paths. [DOI: 10.1115/1.4006266]

Keywords: automatic mechanism synthesis, spring-connected block model, optimization, numerical instability

1 Introduction

This investigation is a follow-up research of the earlier work [1] on the automatic synthesis of planar path generation mechanisms. Here, automatic synthesis implies the synthesis of a linkage mechanism that converts a given input motion to a desired output motion without using any baseline linkage such as a four-bar linkage. If a specific linkage type that is selected at the beginning of the synthesis cannot produce the target motion, it would be impossible to find the desired linkage mechanism. Therefore, an automatic synthesis method that can simultaneously determine the linkage type and its dimensions is envisioned.

Figure 1(a) schematically illustrates a synthesis problem. Within the domain of mechanism design, one should find the type and dimensions of a linkage that converts an input motion to a desired output motion. An important step in Ref. [1] is to discretize the design domain into rigid blocks that are interconnected by zero-length springs of varying stiffness values ($k_{\min} \leq k \leq k_{\max}$, k : spring stiffness), as illustrated in Fig. 1(b). The spring element has horizontal-direction stiffness and vertical-direction stiffness but no stiffness during rotational motion. A more refined mechanism can be obtained by finer discretization. The spring-connected rigid block model (SBM) is employed to facilitate mechanism synthesis, and the problem of finding a mechanism to trace a given path is set up as a problem to minimize the difference between the target path and the current path of SBM. To find the desired mechanism configuration, the spring stiffness is treated as a function of the design variable. The connectivity between blocks and springs is illustrated inside the dotted circle of Fig. 1(b); a generic node, P , connects four neighboring blocks with five springs. Note that an anchoring spring of stiffness k_g is

introduced to express the state of connection between the blocks and the ground. Depending on the values of the spring stiffnesses, different linkage states can be realized as illustrated in Fig. 1(c). A spring of stiffness k_{\max} connecting two adjacent blocks simulates a pinned joint; on the other hand, a spring of stiffness k_{\min} connecting two adjacent blocks simulates a disconnected joint. Because a spring having an intermediate stiffness value should not appear at the end of the mechanism synthesis, either an explicit or an implicit condition to push the value of k to either k_{\min} or k_{\max} is implemented in the optimization formulation. Figure 2(a) demonstrates the equivalence between a standard four-bar linkage and an SBM having appropriate spring-stiffness values. As demonstrated in Fig. 2(b), the SBM in Fig. 2(a) follows exactly the same path as the standard four-bar linkage, as the input rotation angle, $\phi_A(t) = \pi t/3$, at A is varied between $t_0 = 0.0$ s and $t_f = 1.5$ s.

To find a linkage mechanism for converting a given input motion at A to a target output motion at Q in Fig. 1(a), the following optimization problem based on SBM was set up by Kim et al. [1]:

$$\underset{\xi \in \mathbb{R}^{N_S}}{\text{Minimize}} \left\{ F = \max_{t_0 \leq t \leq t_f} [\mathbf{r}_Q(t) - \hat{\mathbf{r}}_Q(t)]^2 \right\} \quad (1)$$

Design variables:

$$\xi = \{\xi_1, \xi_2, \xi_3, \dots, \xi_{N_S}\}^T \quad (2)$$

$$k_i = f(\xi_i) \quad (i = 1, 2, 3, \dots, N_S) \quad (3)$$

with

$$0 < k_{\min} \leq k_i \leq k_{\max} \quad (4)$$

where $\mathbf{r}_Q(t)$ is the position vector of the output point Q of the current mechanism design and $\hat{\mathbf{r}}_Q(t)$ is the target position of Q . The spring stiffness, k_i , is varied as a function of the design variable, ξ_i ,

¹Corresponding author.

Contributed by the Mechanisms and Robotics Committee of ASME for publication in the JOURNAL OF MECHANICAL DESIGN. Manuscript received September 2, 2011; final manuscript received February 21, 2012; published online April 3, 2012. Associate Editor: Hong-Sen Yan.

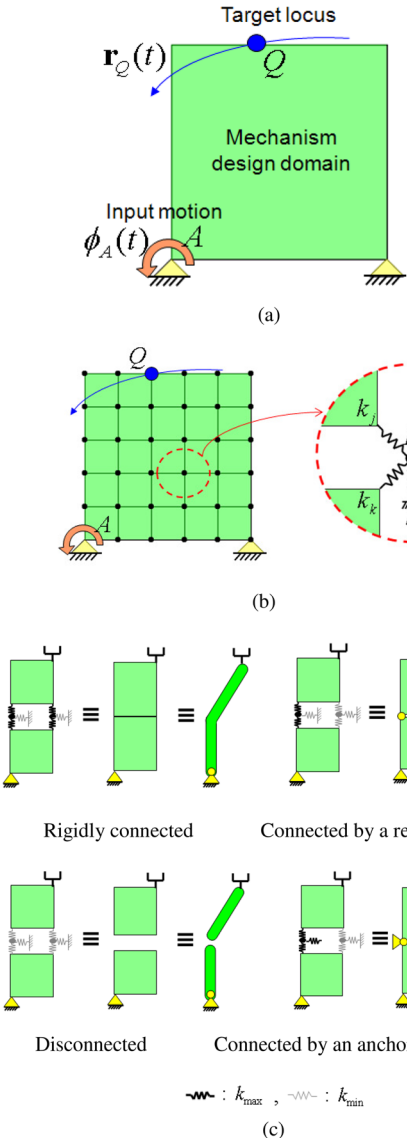


Fig. 1 Overview of the automatic linkage-mechanism synthesis in Ref. [1]: (a) problem definition to find a planar linkage mechanism for converting a given input motion to a desired output motion without relying on any baseline linkage; (b) design domain discretized by spring-connected rigid blocks; and (c) linkage-connection simulation by using SBMs with different spring-stiffness values (k_{\max} : maximum (strong) spring stiffness, k_{\min} : minimum (very weak) spring stiffness)

which is assigned to each of the N_S springs. The function, f , in Eq. (3) should be so selected as to yield distinct states of either $k_i = k_{\min}$ or $k_i = k_{\max}$ at the end of optimization. For all simulations with SBM, the stiffness is normalized such that $k_{\min} = \varepsilon = 10^{-9}$ and $k_{\max} = 1$ (dimensionless quantities will be used without loss of generality). Typically, $f(\xi)$ is selected to be either ξ^p (p : penalty parameter) or an S-shaped function of ξ [2,3]. Once the optimization process is completed, a linkage mechanism corresponding to the optimized SBM can be identified (see Ref. [1]).

Before discussing the numerical issues that arise in the expansion of the aforementioned synthesis method to more general problems, let us review the earlier efforts to synthesize a mechanism without specifying the type of baseline linkage. Chiou and Kota [4] presented a synthesis method based on a matrix representation. They created a mechanism by using a finite set of kinematic building blocks. Lipson and Pollack [5] and Pollack and Lipson [6] used an evolutionary approach to synthesize robotic

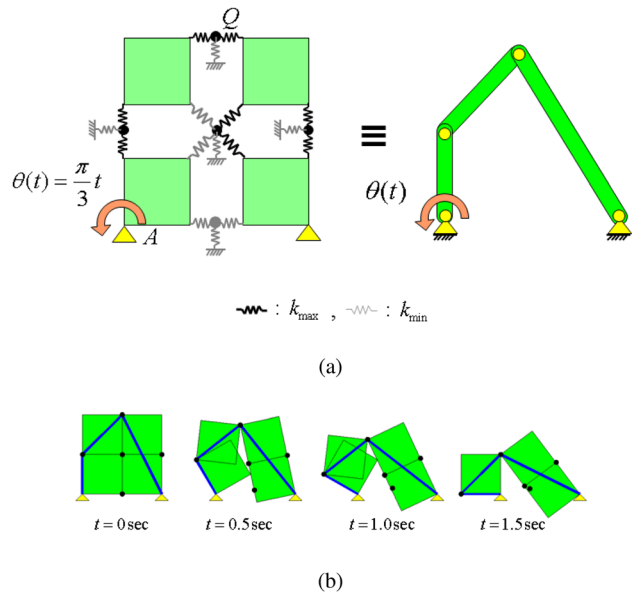
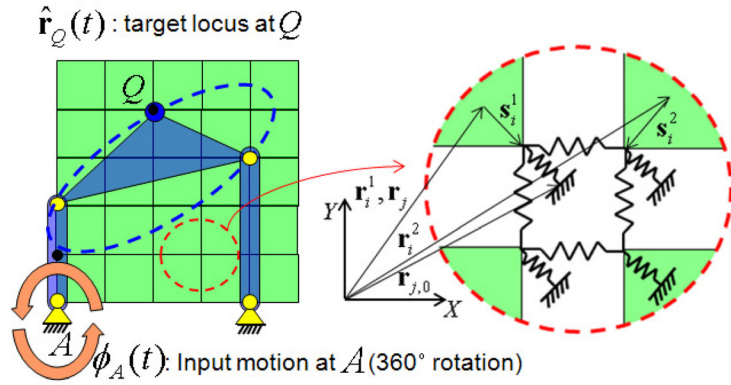


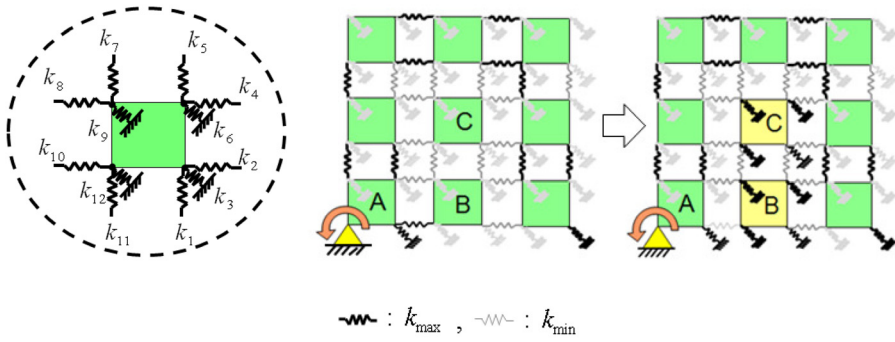
Fig. 2 (a) A four-bar linkage modeled by SBM. (b) The motion of the SBM in (a).

life forms composed of linear actuators, bars, and joints. Fernández-Bustos et al. [7] used the finite element method for kinematic analysis and presented a synthesis method based on a genetic algorithm. In Sedlaczek et al. [8], the fitness of each candidate mechanism for a genetic algorithm was accurately evaluated by dimensional synthesis. Some attempts were also made to use gradient-based optimization techniques. Kawamoto et al. [9] dealt with the design of an articulated mechanism using a truss-based ground-structure representation. Ohsaki and Nishiwaki [10] presented a two-stage optimization approach for generating link mechanisms from a ground structure. Classical synthesis approaches starting with a predetermined mechanism type can be found in Refs. [11–14]. The use of spring-connected rigid links can be found in the analysis and synthesis of compliant mechanisms [15–18]; springs are attached at a rigid link mechanism, and the stiffness values of the springs and the pin joint locations are determined to accurately derive the force–displacement relationship of a compliant mechanism. Nevertheless, the synthesis problems studied in Ref. [1] appear to be difficult to solve by the techniques developed in the aforementioned investigations.

In Ref. [1], relatively simple open-path output trajectories were considered under rotational input motions. On the other hand, this investigation is concerned with mechanism synthesis that can handle complex output trajectories including closed loops. Because no baseline linkage is to be used for the synthesis, an optimization-based formulation using SBM can be employed. When the formulation developed in Ref. [1] was directly applied to closed-loop problems, several numerical instabilities were encountered, such as singularities that arose in the process of solving SBM-based equilibrium equations and deficiency or redundancy in degrees of freedom. Therefore, a modified SBM-based formulation needs to be developed; otherwise, it would be nearly impossible to synthesize more general planar linkages with the SBM approach. Section 2 describes the numerical difficulties of the formulation of Ref. [1] in applying it to more general synthesis problems. Then, an alternative formulation and techniques are presented to resolve these major numerical difficulties. In Sec. 3, the synthesis method based on the alternative formulation is outlined and a procedure to solve the equilibrium equations of SBM is briefly given. Several benchmark-type linkage synthesis problems are investigated to check the effectiveness of the proposed formulation. The findings from this research are summarized in the concluding section.



(a)



(b)

(c)

Fig. 3 (a) The modified SBM proposed in this work. **(b)** A block surrounded by 12 springs. **(c)** An example of floating-block anchoring.

2 Techniques to Resolve Possible Numerical Difficulties

2.1 A Technique to Alleviate Numerical Singularity. The formulation in Ref. [1] determines the spatial locations of rigid blocks by minimizing the potential energy stored in the springs. If rigid blocks or generic nodes are surrounded by only weak springs (having stiffness values close to k_{\min}), the system equilibrium equation can be almost singular because these blocks become virtually unsupported. The blocks connected with only weak springs will be referred to as “floating” blocks. On the other hand, a block that is used to transfer motion will be called a skeletal block. When a target path is relatively short as in Ref. [1], the singularity issue may not appear. In the present problem where the target path is long, i.e., a closed loop, however, floating blocks can cause numerical problems like singularity. To overcome the singularity problem, a technique to anchor the floating blocks to the ground by using the modified model of SBM is proposed, as depicted in Fig. 3(a). Unlike the original SBM of Ref. [1], every corner of each block in the modified SBM can be directly connected to the ground by an anchoring spring. In addition, the blocks can be directly connected to each other. Since no generic point is introduced in the modified model, the total number of degrees of freedom used to discretize a design domain is smaller than that used in the original SBM.

To determine whether a block should be a floating one or not, the springs of stiffness, k_1 to k_{12} illustrated in Fig. 3(b), that are connected to the block are considered. Depending on the stiffness value, the so-called floating block index, I_F , is defined

$$I_F \equiv \sum_{n=1}^4 C_{3n-2} \vee C_{3n-1} \vee C_{3n} \quad (5a)$$

$$C_i = \begin{cases} 1 & (\text{connected}) \quad \text{if } k_i \geq \delta \\ 0 & (\text{disconnected}) \quad \text{if } k_i < \delta \end{cases} \quad (5b)$$

where n is an index representing the location of the n th corner of a block and the symbol, \vee , denotes the logical “or” operator for bitwise operation. The following is the criterion to determine the block state:

If $I_F \geq 2$, the block is a skeletal block (it transfers motion).

If $I_F = 0$ or 1, the block is declared as a floating block and is anchored to the ground by setting k_{3n-2} , $k_{3n-1} = k_{\min}$, and $k_{3n} = k_{\max}$ ($n = 1, 2, 3, 4$).

The above criterion states that the translational degree of a corner point in a rigid block is regarded to be constrained if more than one spring (among the three springs) has a stiffness value larger than δ (a typical value of $\delta = 10^{-3}$ is used). It also states that a block with $I_F \geq 2$, i.e., a block having two or more corners connected to the neighboring blocks or the ground, is declared as a skeletal block. On the other hand, a block with $I_F = 0$ or 1 is declared as a floating block and will be anchored to the ground. Even if a floating block is anchored, the output motions before and after anchoring will be virtually the same. In actual numerical implementation, one can make an additional check on the proper selection of floating blocks. If the motions before and after anchoring are considerably different, the block should be treated as a skeletal block.

An example of floating-block anchoring is illustrated in Fig. 3(c) where the floating blocks, Blocks B and C, are anchored to the ground. Because Block B having $I_F = 1$ can freely rotate around the lower-right corner of Block A, it is a floating block that should be anchored. Block C is also a floating block because it can freely rotate and translate in all directions. As shown in the illustration on the right in Fig. 3(c), all of the ground springs are set to have the

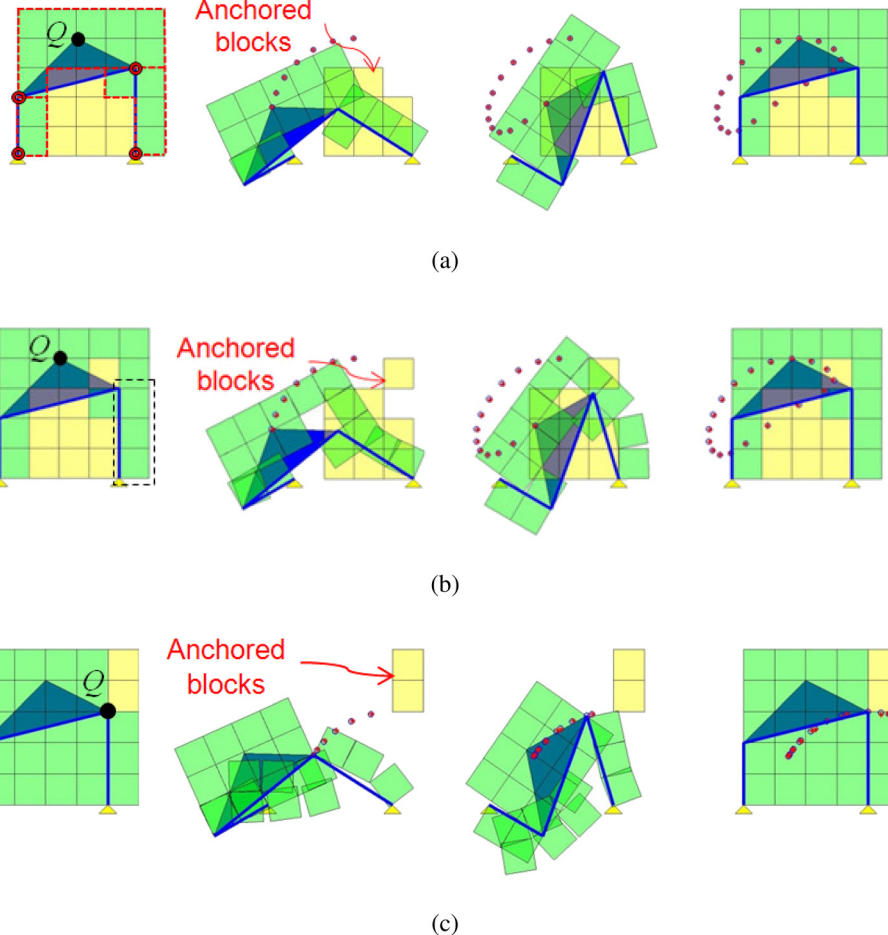


Fig. 4 Motions of SBMs having (a) proper degrees of freedom, (b) redundant degrees of freedom, and (c) deficient degrees of freedom (*: current path of the output point, o: target path)

maximum stiffness ($k_{3n} = k_{\max}$, $n = 1, 2, 3, 4$) to represent anchoring.

2.2 A Technique to Ensure Proper Number of Degrees of Freedom at the Final Stage. In this section, the issue related to the kinematic degree of freedom of the original SBM is examined and a technique to overcome the problems related to the kinematic degree of freedom is suggested. For the discussion, consider Fig. 4(b) in which the synthesized block configuration accurately traces the desired motion. However, it is not possible to extract a corresponding rigid planar linkage from the block model. For instance, one can extract a meaningful linkage from the snapshots in Fig. 4(b), while one can extract a rigid planar linkage from the second and third snapshots in Fig. 4(a). Specifically, let us consider the three blocks marked inside the dotted line in Fig. 4(b). If the blocks are connected by rigid hinge joints, the block system has redundant degrees of freedom (DOFs) because the three rigid blocks are serially connected through two hinge joints. In this instance, the spatial positions of the three blocks cannot be uniquely determined during the motion of the mechanism. Since the blocks are connected by elastic springs, however, their positions can be calculated without any singularity by minimizing the total potential energy of the spring system (this solution process will be explained in Sec. 3). Conversely, the resulting SBM that is deficient in degrees of freedom can produce the desired motion if the applied torque at the input link is sufficiently large because the springs with $k_i \cong k_{\max}$ can still elastically deform. Figure 4(c) shows the case in consideration. From this study, redundancy or deficiency in DOFs occurs because a kinematic problem is simulated as a static equilibrium problem for the SBM approach.

When an SBM has insufficient DOFs, the strain energy of the SBM becomes very large when it moves. For example, the strain energy stored in all springs in Fig. 4(c) is $S = 30.555$ at a certain time-step, while the energy in Fig. 4(a) is $S \cong 10^{-3}$. This result implies that the strain energy of an SBM during movement should be constrained to avoid insufficient DOFs. On the other hand, the SBM would not have large strain energy during movement (the value of $S = 0.0214$ was observed in the case of the model in Fig. 4(b)) if it has redundant DOFs. Therefore, strain energy cannot be used to control DOF redundancy. Since SBM having redundant DOFs cannot keep its shape even under a small external force, it will undergo a large displacement under a moderately large external force. Thus, the DOF redundancy issue can be resolved by minimizing the displacement under artificial external forces.

3 Proposed Formulation for Mechanism Synthesis

3.1 Alternative Optimization Formulation. Based on the findings from Sec. 2, the following optimization formulation is proposed to synthesize a planar mechanism that traces a target path at the output point:

For $n_k = n_1, n_2, \dots, N_T$, repeat

$$\underset{\xi \in \mathbb{R}^N}{\text{Minimize}} F = (1 - w) \frac{S}{S_0} + w \frac{D}{D_0}, \quad (0 \leq w \leq 1) \quad (6a)$$

$$\text{subject to } G_j = (\mathbf{r}_Q(t_j) - \hat{\mathbf{r}}_Q(t_j))^T (\mathbf{r}_Q(t_j) - \hat{\mathbf{r}}_Q(t_j)) \leq \varepsilon^2, \quad (6b)$$

for $j = 0, \dots, n_k$

with

$$S = \sum_{j=1}^{N_T} \sum_{i=1}^{N_S} \frac{1}{2} \mathbf{U}_i^T(t_j) \mathbf{K}_i \mathbf{U}_i(t_j) \quad (6c)$$

$$D = \left[(\mathbf{P}_o^{F_x} - \mathbf{P}_o)^2 + (\mathbf{P}_o^{F_y} - \mathbf{P}_o)^2 \right] \Big|_{t=t_0} \quad (6d)$$

where N_T is the number of time-steps for an analysis. In Eq. (6a), two kinds of compliance are considered: the compliance S due to an input motion introduced to prevent DOF deficiency and the compliance D due to artificial external loads introduced to prevent DOF redundancy. The latter is expressed indirectly in terms of the squared distance between the positions before and after the load application. Similar ideas were effective in the topology optimization problems of compliant mechanisms [19–21]. In a compliant mechanism design, gray elements appearing during the synthesis process may be regarded to act as redundant degrees of freedom. To suppress the appearance of the gray elements, the system compliance due to an input force is constrained to be smaller than a prescribed value [19,20] or is minimized [21]. In the case of a path-generating compliant mechanism [19], artificial external loads were used to maintain the stiffness of the designed mechanism. Unlike a compliant mechanism design, a spring connected to a block can act as a revolute joint only when the other springs connected to the same block have the stiffness values as explained earlier. Therefore, in the SBM approach, a mechanism having proper number of DOFs can be synthesized by considering the system compliances. The subscript, 0, in Eq. (6) denotes the initial model, and w is a weighting parameter. In Eq. (6c), N_S is the number of springs while \mathbf{U}_i and \mathbf{K}_i denote the deformation vector of spring i and its stiffness matrix, respectively. The variable D in Eqs. (6a) and (6d) denotes the squared distance between the posi-

tion, \mathbf{P}_o , of the center of the output block before the application of the artificial forces and its displaced positions, $\mathbf{P}_o^{F_x}$ and $\mathbf{P}_o^{F_y}$, after the application of horizontal and vertical artificial forces, respectively. The value of D is calculated only at the first time-step of a given SBM configuration.

Along with the formulation in Eq. (6), the stiffness of the elastic spring that connects the rigid blocks is penalized as

$$k_i = f(\xi_i) = \xi_i^p \quad (i = 1, \dots, N_S) \quad (7)$$

The penalization helps to push the design variable, ξ_i , toward either its lower or upper bound [1]. When a strain energy term such as S appears in the objective function, the polynomial penalization ($p > 1$) (the value of $p = 3$ is used in this work) effectively pushes the value of ξ_i to its upper or lower bound [2]. Consequently, one can extract a linkage mechanism from an optimized SBM configuration without ambiguity.

To circumvent numerical difficulties in SBM that result from the high nonlinearity of the optimization problem, multiple minimization problems are continuously solved as time increases. After a mechanism following the first part of a target path between $t = t_0$ and $t = t_{n_1}$ is found within an error of ε , the mechanism is reoptimized to follow the extended target path between $t = t_0$ and $t = t_{n_2}$ as the next optimization problem. In this strategy, the optimized mechanism of the current optimization problem is used as the initial guess for the next optimization problem. This process is repeated until n_k becomes N_T to cover the given target path, long or closed.

To solve the minimization problem defined in Eq. (6), the method of moving asymptotes (MMA) [22], a gradient-based optimizer, is used. The sensitivities of the objective function and the constraint equations that should be supplied for MMA will be derived in the later part of this section. The overall procedure to solve Eq. (6) is outlined in Fig. 5.

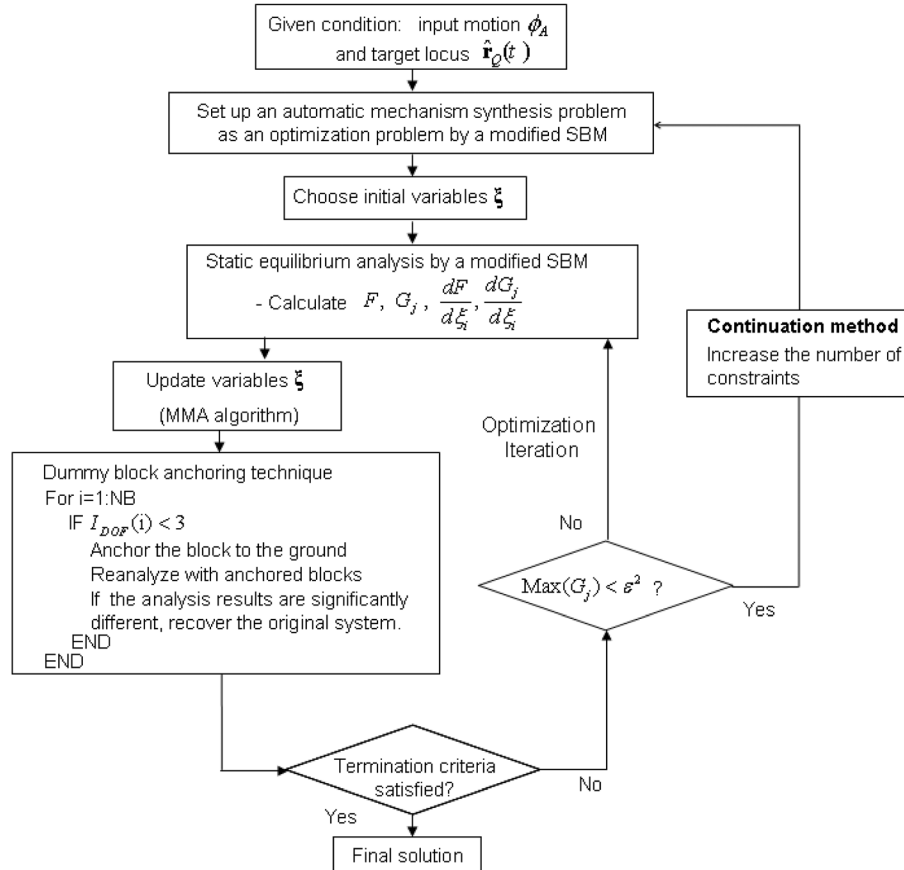


Fig. 5 Flowchart of the optimization process using the proposed formulation

3.2 Equilibrium Analysis. To find the spatial positions of blocks at every time-step of motion for a given SBM configuration, one can minimize the total strain energy of the SBM system

$$\begin{aligned} \text{Minimize}_{\mathbf{q} \in \mathbb{R}^{3N_B}} V(\mathbf{q}) = & \frac{1}{2} \sum_{i=1}^{N_{CS}} k_i (\mathbf{r}_i^1 + \mathbf{A}_i^1 \mathbf{s}_i^1 - \mathbf{r}_i^2 - \mathbf{A}_i^2 \mathbf{s}_i^2)^T \\ & (\mathbf{r}_i^1 + \mathbf{A}_i^1 \mathbf{s}_i^1 - \mathbf{r}_i^2 - \mathbf{A}_i^2 \mathbf{s}_i^2) \\ & + \frac{1}{2} \sum_{j=1}^{N_{AS}} \left\{ k_j (\mathbf{r}_j + \mathbf{A}_j \mathbf{s}_j - \mathbf{r}_{j,0})^T (\mathbf{r}_j + \mathbf{A}_j \mathbf{s}_j - \mathbf{r}_{j,0}) \right\} \end{aligned} \quad (8a)$$

subject to

$$\phi_A = \phi^* \quad \text{at a given time-step } t = t^* \quad (8b)$$

with

$$\mathbf{q} = \left\{ \mathbf{q}_1^T, \mathbf{q}_2^T, \dots, \mathbf{q}_{N_B}^T \right\}^T, \quad \mathbf{q}_l = \left\{ \mathbf{r}_l^T, \phi_l \right\}^T = \left\{ x_l, y_l, \phi_l \right\}^T, \text{ and}$$

$$\mathbf{A}_l = \begin{bmatrix} \cos \phi_l & -\sin \phi_l \\ \sin \phi_l & \cos \phi_l \end{bmatrix} \quad (8c)$$

In Eq. (8a), N_{CS} , N_{AS} , and N_B denote the numbers of block-connecting springs, anchoring springs, and rigid blocks, respectively. The symbols \mathbf{r}_i^1 and \mathbf{r}_i^2 , respectively, denote the coordinates of the centers of two blocks connected with spring i (a superscript 1 is used to distinguish the two connected blocks), while \mathbf{s}_i^1 and \mathbf{s}_i^2 , the position vectors from the centers of the two blocks to spring i , and \mathbf{A}_i^1 and \mathbf{A}_i^2 , the rotation matrices of the two blocks. The coordinates of the anchoring spring j are expressed by using the coordinates of the center of the block connected with the anchoring spring (\mathbf{r}_j), the position vector from the center of the block to the anchoring spring (\mathbf{s}_j), and the rotation matrix of the block (\mathbf{A}_j). Note that only one block is connected to an anchoring spring. In Eq. (8a), $\mathbf{r}_{j,0}$ indicates the anchoring point of spring j , which is fixed during the motion of the mechanism. The rotational angle of the block where an input motion is imposed is denoted by ϕ_A . In Eq. (8c), \mathbf{q}_l indicates the position of block l .

The minimization problem in Eq. (8) can be rewritten as an unconstrained minimization problem by excluding the position of the block under the input motion, $\mathbf{q}_A = \{x_A, y_A, \phi_A\}^T$

$$\text{Minimize}_{\mathbf{v} \in \mathbb{R}^{3N_B-3}} V(\mathbf{v}) \quad (9)$$

where $\mathbf{v} = \mathbf{q} - \mathbf{q}_A$. The solution of Eq. (9) can be found from the condition that the derivative of the total strain energy with respect to \mathbf{v} vanishes

$$\frac{dV}{d\mathbf{v}} = 0 \quad (10)$$

Equation (10) can be solved by using the iterative Newton-Raphson scheme

$$\mathbf{v}^{k+1} = \mathbf{v}^k - \mathbf{J}^{-1} \frac{dV}{d\mathbf{v}} \Big|_{\mathbf{v}=\mathbf{v}_k} \quad (11a)$$

where the Jacobian matrix \mathbf{J} is defined as

$$\mathbf{J} = \frac{d}{d\mathbf{v}} \left(\frac{dV}{d\mathbf{v}} \right) \quad (11b)$$

3.3 Sensitivity Analysis. The sensitivity of the objective function in Eq. (6a) with respect to the design variable, ξ_i , is

$$\begin{aligned} \frac{dF}{d\xi_i} &= \frac{dF}{dk_i} \frac{dk_i}{d\xi_i} = \left[\frac{(1-w)}{S_0} \frac{dS}{dk_i} + \frac{w}{D_0} \frac{dD}{dk_i} \right] \frac{dk_i}{d\xi_i} \\ &= \frac{(1-w)}{S_0} p \xi_i^{p-1} \sum_{j=1}^{N_T} \sum_{i=1}^{N_S} \frac{1}{2} \left[2 \frac{d\mathbf{U}_i^T(t_j)}{dk_i} \mathbf{K}_i \mathbf{U}_i(t_j) + \mathbf{U}_i^T(t_j) \mathbf{U}_i(t_j) \right] \\ &\quad + \frac{w}{D_0} p \xi_i^{p-1} \left[\frac{d(\mathbf{P}_o^{F_x} - \mathbf{P}_o)}{dk_i} + \frac{d(\mathbf{P}_o^{F_y} - \mathbf{P}_o)}{dk_i} \right] \end{aligned} \quad (12)$$

Here, $d\mathbf{U}_i/dk_i$ is written as

$$\begin{aligned} \frac{d\mathbf{U}_i}{dk_i} &= \frac{\partial \mathbf{U}_i}{\partial x_i^1} \frac{\partial x_i^1}{\partial k_i} + \frac{\partial \mathbf{U}_i}{\partial y_i^1} \frac{\partial y_i^1}{\partial k_i} + \frac{\partial \mathbf{U}_i}{\partial \phi_i^1} \frac{\partial \phi_i^1}{\partial k_i} + \frac{\partial \mathbf{U}_i}{\partial x_i^2} \frac{\partial x_i^2}{\partial k_i} + \frac{\partial \mathbf{U}_i}{\partial y_i^2} \frac{\partial y_i^2}{\partial k_i} \\ &\quad + \frac{\partial \mathbf{U}_i}{\partial \phi_i^2} \frac{\partial \phi_i^2}{\partial k_i} \end{aligned} \quad (13)$$

The symbols $\{x_i^1, y_i^1, \phi_i^1\}$ and $\{x_i^2, y_i^2, \phi_i^2\}$ denote the positions of the blocks connected to spring i . For the design variable attached to an anchoring spring, Eq. (13) should be modified to consider only one block. The expressions $\partial \mathbf{U}_i/\partial x_i$, $\partial \mathbf{U}_i/\partial y_i$, and $\partial \mathbf{U}_i/\partial \phi_i$ are vectors, which are equal to zero, except for those corresponding to the components x_i , y_i , and ϕ_i , respectively, and $\partial x_i/\partial k_i$, $\partial y_i/\partial k_i$, and $\partial \phi_i/\partial k_i$ are obtained by differentiating Eq. (10)

$$\frac{d}{dk_i} \left(\frac{\partial V}{\partial \mathbf{v}} \right) = \frac{\partial}{\partial k_i} \left(\frac{\partial V}{\partial \mathbf{v}} \right) + \frac{\partial}{\partial \mathbf{v}} \left(\frac{\partial V}{\partial k_i} \right) = \frac{\partial}{\partial k_i} \left(\frac{\partial V}{\partial \mathbf{v}} \right) + \mathbf{J} \frac{\partial \mathbf{v}}{\partial k_i} = 0 \quad (14a)$$

$$\frac{\partial \mathbf{v}}{\partial k_i} = -\mathbf{J}^{-1} \frac{\partial}{\partial k_i} \left(\frac{\partial V}{\partial \mathbf{v}} \right) \quad (14b)$$

Note that the decomposition of the Jacobian matrix, \mathbf{J} , in Eq. (14b) already has been performed in the process of solving the equilibrium equation in Eq. (11a).

The derivatives, with respect to the stiffness variable appearing in Eq. (12), of the squared distances $((\mathbf{P}_o^{F_x} - \mathbf{P}_o)^2$ and $(\mathbf{P}_o^{F_y} - \mathbf{P}_o)^2$) between \mathbf{P}_o (the center of the output block before the application of the artificial forces) and its displaced positions, $\mathbf{P}_o^{F_x}$ and $\mathbf{P}_o^{F_y}$, after the application of horizontal and vertical artificial forces, are written as

$$\begin{aligned} \frac{d(\mathbf{P}_o^{F_x} - \mathbf{P}_o)^2}{dk_i} &= 2(\mathbf{P}_o^{F_x} - \mathbf{P}_o)^T \frac{d\mathbf{P}_o^{F_x}}{dk_i} \\ &= 2(\mathbf{P}_o^{F_x} - \mathbf{P}_o)^T \left(\frac{\partial \mathbf{P}_o^{F_x}}{\partial x_o} \frac{\partial x_o}{\partial k_i} + \frac{\partial \mathbf{P}_o^{F_x}}{\partial y_o} \frac{\partial y_o}{\partial k_i} + \frac{\partial \mathbf{P}_o^{F_x}}{\partial \phi_o} \frac{\partial \phi_o}{\partial k_i} \right) \end{aligned} \quad (15a)$$

$$\begin{aligned} \frac{d(\mathbf{P}_o^{F_y} - \mathbf{P}_o)^2}{dk_i} &= 2(\mathbf{P}_o^{F_y} - \mathbf{P}_o)^T \frac{d\mathbf{P}_o^{F_y}}{dk_i} \\ &= 2(\mathbf{P}_o^{F_y} - \mathbf{P}_o)^T \left(\frac{\partial \mathbf{P}_o^{F_y}}{\partial x_o} \frac{\partial x_o}{\partial k_i} + \frac{\partial \mathbf{P}_o^{F_y}}{\partial y_o} \frac{\partial y_o}{\partial k_i} + \frac{\partial \mathbf{P}_o^{F_y}}{\partial \phi_o} \frac{\partial \phi_o}{\partial k_i} \right) \end{aligned} \quad (15b)$$

where $\{x_o, y_o, \phi_o\}$ denotes the position of the output block. The position vectors $\mathbf{P}_o^{F_x}$ and $\mathbf{P}_o^{F_y}$ are calculated from static equilibrium analysis after artificial forces are applied. The adjoint variable method commonly used in structural optimization problems [19] is employed to calculate $\partial x_o/\partial k_i$, $\partial y_o/\partial k_i$, and $\partial \phi_o/\partial k_i$.

Finally, the sensitivity of the constraint is

$$\frac{dG_j}{d\xi_i} = 2p \xi_i^{p-1} (\mathbf{r}_Q(t_j) - \hat{\mathbf{r}}_Q(t_j))^T \frac{d\mathbf{r}_Q(t_j)}{dk_i} \quad (16)$$

where $d\mathbf{r}_Q(t_j)/dk_i$ is available from the solution of Eq. (14b).

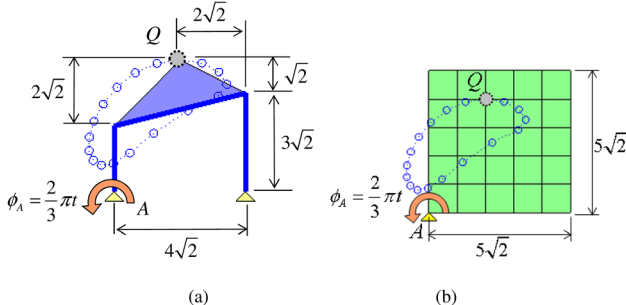


Fig. 6 Linkage-mechanism synthesis problem: (a) a target mechanism having a closed path and (b) the employed SBM discretized by 5×5 blocks

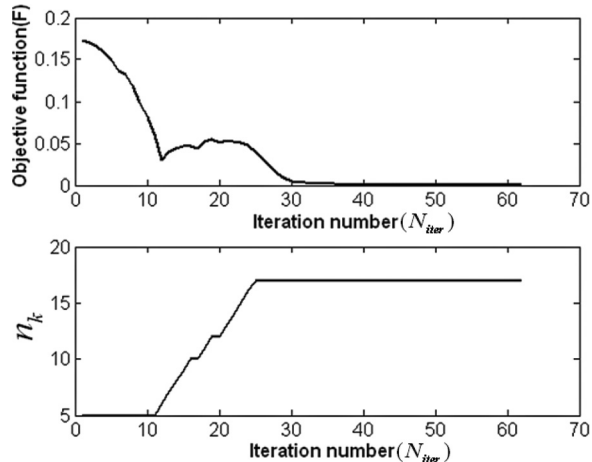


Fig. 7 Iteration histories of the objective function, F , and the value of n_k for the synthesis problem in Fig. 6

4 Case Studies

The first case study is to check whether a known four-bar linkage mechanism shown in Fig. 6(a) can be found by the proposed formulation. Figure 6(b) shows the employed SBM discretized by 5×5 rigid blocks. These blocks are interconnected by 80 block-connecting springs and have 99 anchoring springs. The input block rotates at $\phi_A(t) = 2\pi t/3$ with its lower-left corner fixed. The target path, $\hat{r}_Q(t)$, represents a closed loop. Because the path of the SBM is found by solving the static governing equation in Eq. (10), the discretization accuracy of the target path is important, and not the angular velocity of the input block, in the present problem. The target paths in all the examples considered in this work are depicted by the points on the paths determined for every 20 deg of the input angle, so that a total of 18 points are used to measure the distance between the target paths and the current paths realized by the SBM during optimization. With this level of discretization, a target path can be sufficiently accurately represented.

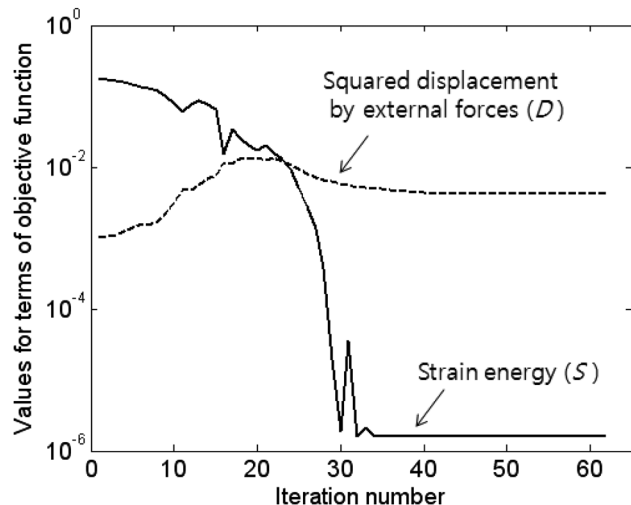


Fig. 8 Iteration history for the strain energy, S , and the squared displacement by external forces, D

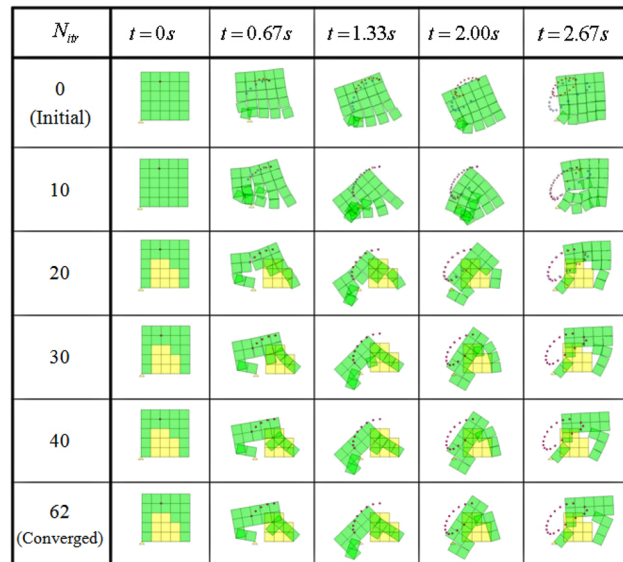


Fig. 9 Output paths of the intermediate and final SBMs for the synthesis problem in Fig. 6

sented. Denser discretization, which requires a large number of static analyses in Eq. (10), is avoided. Numerical tests indicated that improvements were marginal. The application of the earlier formulation in Ref. [1] failed to yield the correct solution because it could not handle a long path problem. The appropriate orders of

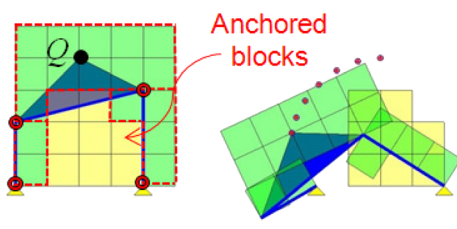


Fig. 10 Motions of the converged SBM and the identified linkage mechanism for the synthesis problem in Fig. 6

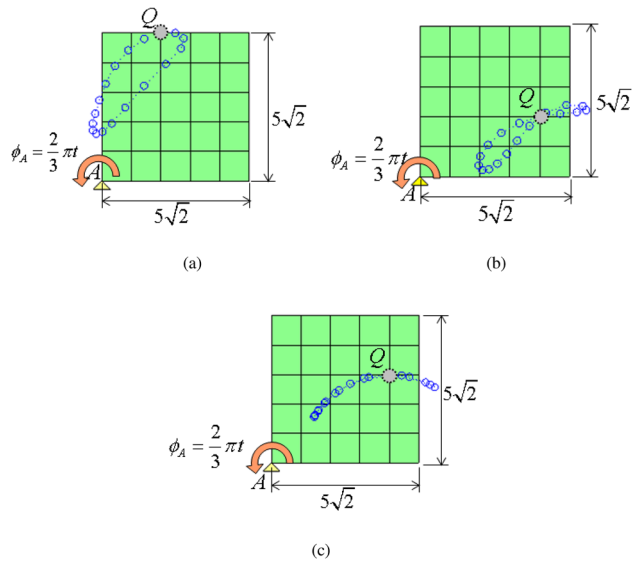


Fig. 11 Definitions of synthesis problems having different paths at the output point, Q

magnitude of parameters such as w are determined by numerical tests; the values of $w = 0.001$ and $\varepsilon = 0.2$ are selected and also the magnitudes of the artificial forces of $F_x = F_y = 0.01$ are chosen. These values are used throughout the present investigation.

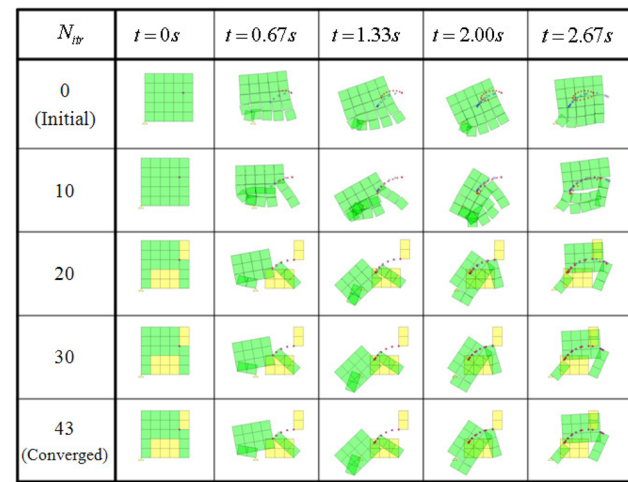


Fig. 13 Motion histories at several iterations for the problem defined in Fig. 10(c)

Because many local minima can appear in nonlinear optimization problems, the initial design variables obviously will affect solution convergence. When the initial values of the anchoring springs were uniformly set to $k_A = k_{min}$, the optimizer yielded an incorrect open linkage. To avoid this problem, one of the blocks was arbitrarily anchored to form a closed linkage at the beginning

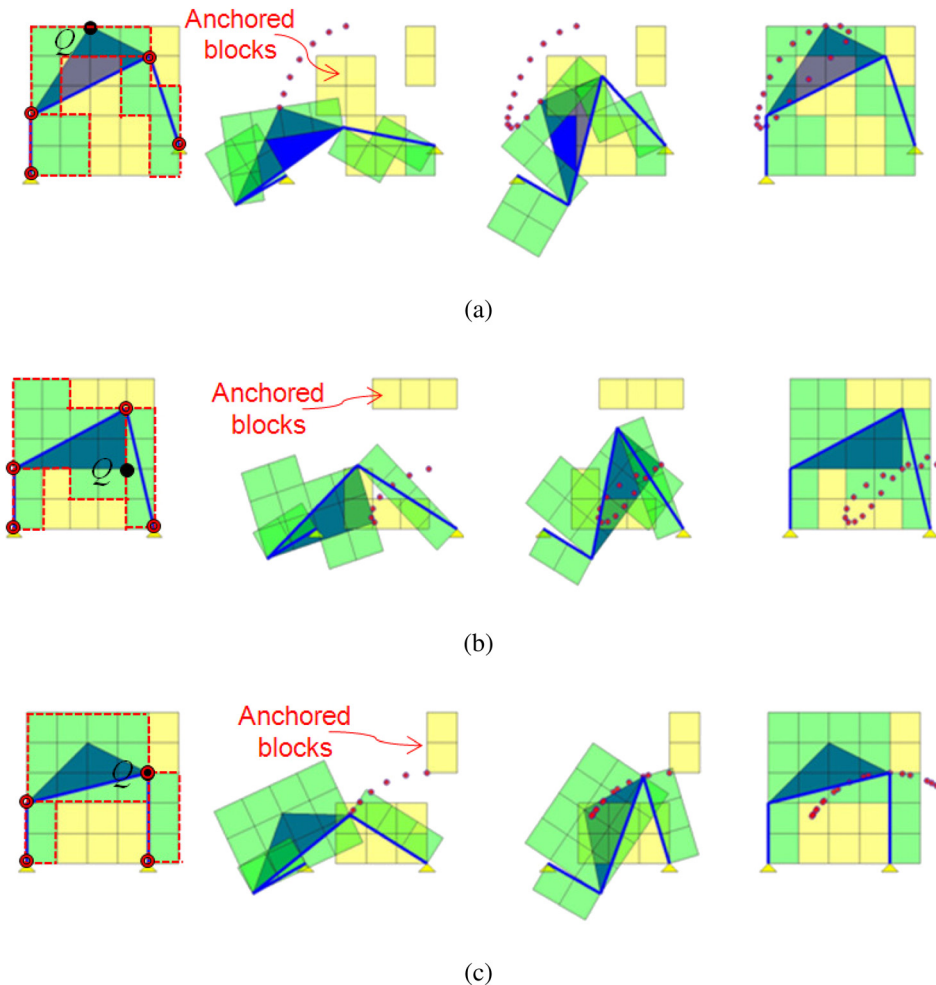


Fig. 12 Comparison between the output motions of the converged SBMs and those of the identified linkage mechanisms for the synthesis problems in (a) Fig. 10(a), (b) Fig. 10(b), and (c) Fig. 10(c)

of the optimization, and the anchoring position was changed by optimization during the process. In addition, the initial values of the block-connecting springs were set as $\xi_i = 0.5$ in Eq. (7). The converged result was obtained after 62 iterations. Figure 7 shows the histories of the objective function and the number n_k of constraints. Note that the objective function does not monotonically

converge because the total strain energy also increases with more time-steps in the optimization. In Fig. 8, the iteration histories of the strain energy (S) and the squared distance by external forces (D) are plotted. While the deformation by the external forces does not significantly change, the strain energy stored in the springs decreases to an order of 10^{-5} as the optimization converges.

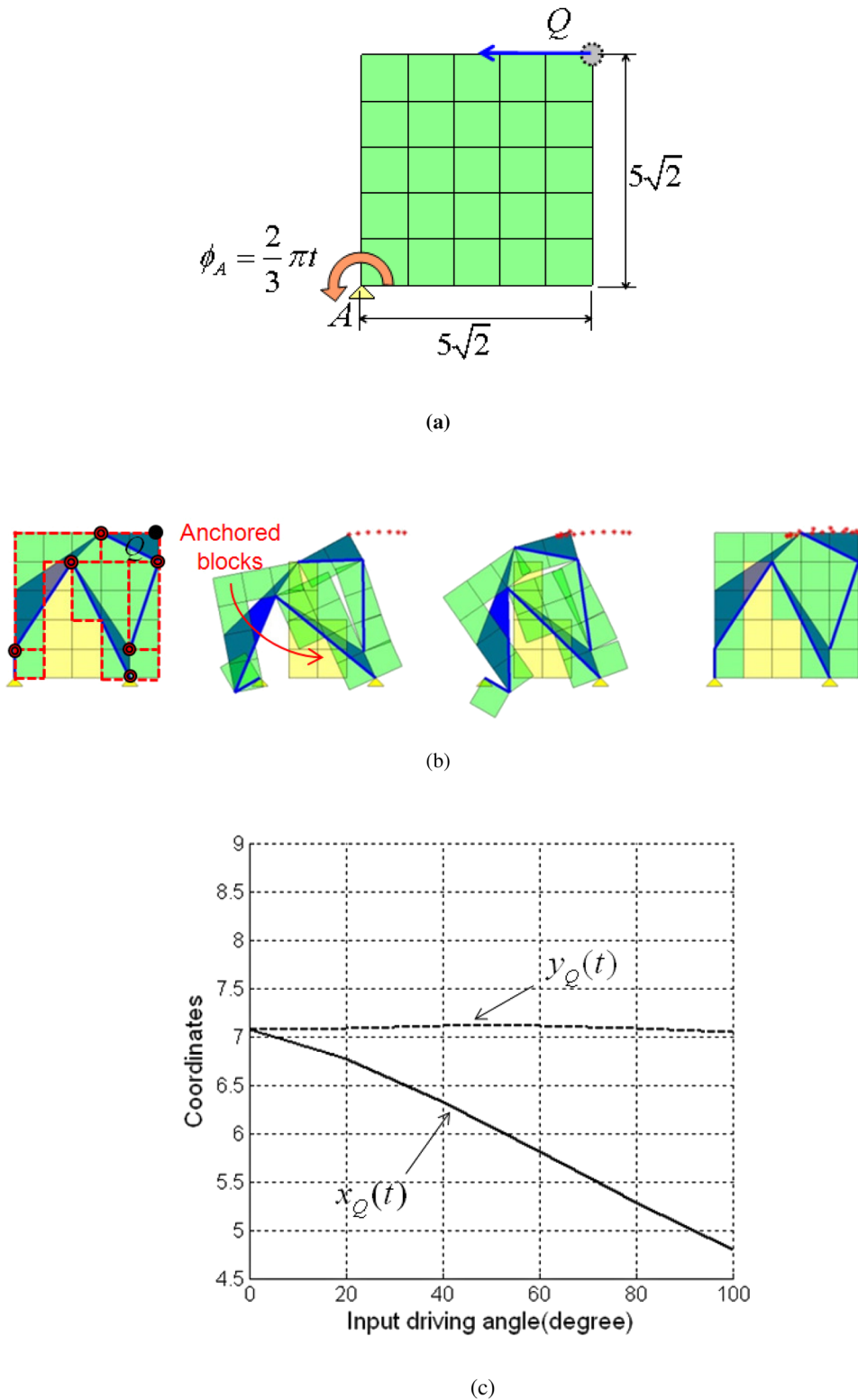


Fig. 14 (a) Problem definition to synthesize a straight-line mechanism by using SBM. (b) Output motions of the converged SBM and the identified six-bar linkage. (c) Path of the output point of the identified mechanism.

Because of this decrease in the strain energy, a small weight parameter $w=0.001$ was employed, and it gave satisfactory solutions for most problems when the initial values of the block-connecting springs were set to $\xi_i = 0.5$.

The output paths of the intermediate and final SBMs are illustrated in Fig. 9 for several iteration steps. The figure shows that while the SBM does not follow the target path at the initial iteration, the output path becomes progressively closer to the target path. Because the static stiffness of the SBM is considered in the objective function, all the springs have stiffness values that are sufficiently close to k_{\min} or k_{\max} at the final iteration step. Consequently, there is no difficulty in identifying an equivalent linkage mechanism from the converged SBM, as demonstrated in Fig. 10. In the first figure of Fig. 10, each set of blocks surrounded by a closed dotted line denotes one rigid link. The joint types in the system can be identified by examining the motions of SBM. Figure 10 shows that the identified linkage mechanism is the same as the one used to produce the target path, $\mathbf{r}_Q(t)$, in Fig. 6(a).

Mechanisms for the other target paths are synthesized, as shown in Fig. 11. Following the same procedure as in the previous problem, the converged SBMs shown in Fig. 12 are obtained. The mechanisms identified from the SBMs are found to be the same as those used to produce the target paths in Fig. 11. Note that depending on the target paths, the anchored blocks are differently selected. Figure 13 illustrates the motions of a mechanism at several iteration steps. The figure shows that all the blocks at the initial step seem to move as a whole, and that the SBM at the 20th iteration traces the target path quite closely while some blocks become anchored.

Next, we attempt to synthesize a mechanism that yields an output motion without explicitly prescribing the output motion as a function of an input motion or time. Figure 14(a) depicts the synthesis problem of a mechanism that converts an input rotation to a leftward straight-line motion between $t = 0$ and $t = t_{N_M}$. After $t = t_{N_M}$, the output point is supposed to return back to its original position along an arbitrary path. The rotational angle, $\phi_A(t)$, at A is given as $\phi_A(t) = 2\pi t/3$ ($0 \leq t \leq 3$), and $t_{N_M} = 0.83$ is used ($\phi_A(t_{N_M}) = 100$ deg). An additional constraint to consider is that the straight horizontal movement should be larger than $l = 2.0$. Although there are some known straight-line mechanisms such as the Peaucellier–Lipkin linkage, it will be interesting to synthesize a path generation mechanism that does not explicitly depend on an input motion.

To solve this problem, the formulation in Eqs. (6) is modified as

For $n_k = n_1, n_2, \dots, N_T$, repeat

$$\underset{\xi \in \mathbb{R}^N}{\text{Minimize}} \quad F = (1-w) \frac{S}{S_0} + w \frac{D}{D_0}, \quad (0 \leq w \leq 1) \quad (17a)$$

$$\text{subject to } G_j = \frac{(y_Q(t_j) - y_Q(t_0))^2}{\varepsilon^2} - 1 < 0 \quad \text{for } j = 1, \dots, L \quad (17b)$$

$$H = (x_Q(t_{N_M}) - x_Q(t_0)) \leq -l \quad (17c)$$

where $L = \min(n_k, N_M)$. Equations (17b) and (17c) constrain the straightness of the output path for $0 \leq t \leq t_{N_M}$ and the length of the straight path, respectively. Figure 14(b) shows the optimized SBM, the identified six-bar mechanism, and its snapshots during motion. Figure 14(c) shows the actual path of the output point. Although the path of the mechanism found by the present technique is not perfectly straight, the present technique can automatically find a mechanism that yields a path close to the straight line from a simplified design domain.

5 Concluding Remarks

This work was focused on expanding the synthesis of an SBM-based planar linkage mechanism to deal with more general output paths such as closed and/or longer paths. For the expansion, two

main limiting numerical issues of deficiency and redundancy in the DOFs of a mechanism were identified and techniques to resolve them were suggested. Although the SBM approach enabled mechanism synthesis without any specific linkage type, the numerical problems were inevitable because of the use of multiple elastic springs. The proposed technique to resolve the DOF issues considered the compliances of the spring system due to an input motion and artificial external loads in the objective function. The minimization of the compliance effectively resolved both the DOF deficiency and redundancy. To deal with longer target paths, a multistage optimization strategy was proposed. In this approach, a mechanism following a part of the target path is searched at the initial stage of the optimization-based synthesis and then the search path is gradually increased until it reaches the full path. Because the mechanism found for the previous path is utilized to find the following increased path, solution convergence can be greatly enhanced. This approach was validated with numerical case studies. Although this study reports an improved SBM approach that can solve a new class of mechanism synthesis problems, several issues still remain to be addressed. The gradient-based approach certainly can deal with a large-sized problem than nongradient approaches, but it has convergence and local minimum issues. To reduce the computational cost and improve solution convergence, one may consider a two-stage synthesis strategy that determines the mechanism type by the proposed method and then adjusts the link lengths and joint locations by a sizing optimization technique. There are also issues in selecting various parameters appearing in the optimization formulation. SBM-based synthesis is still in an early development stage, so it should be studied further before it can be effectively used for the envisioned automatic mechanism synthesis.

Acknowledgment

This work was supported by the National Research Foundation of Korea (NRF) Grant No. 2011-0017445 funded by the Korean Ministry of Education, Science and Technology (MEST) contracted through IAMD at Seoul National University and WCU program (No. R31-2010-000-10083-0) through NRF funded by MEST.

Nomenclature

$\mathbf{A}_i^1, \mathbf{A}_i^2$	= rotation matrices of the two blocks connected with the block-connecting spring i
\mathbf{A}_j	= rotation matrix of the block connected with the anchoring spring j
C_i	= index to denote connection status of spring i
D	= compliance of SBM due to artificial external loads
F	= objective function of the optimization
G_j	= j th constraint of the optimization
I_F	= index to denote the floating status of a block
N_{AS}	= number of anchoring springs
N_B	= number of rigid blocks
N_{CS}	= number of block-connecting springs
N_M	= number of time-steps for a straight-line motion that is a part of a full motion in a straight-line mechanism problem
N_S	= number of total springs ($N_S = N_{CS} + N_{AS}$)
N_T	= number of time-steps for the analysis of a full motion
\mathbf{P}_o^F	= position vector of the center of the output block
$\mathbf{P}_o^{F_x}, \mathbf{P}_o^{F_y}$	= position vectors of the displaced centers of the output block by horizontal and vertical artificial external loads at output point Q
S	= compliance of SBM due to an input motion
k_i	= spring stiffness parameterized with ξ_i ($k_{\min} \leq k_i \leq k_{\max}$)
$\mathbf{r}_i^1, \mathbf{r}_i^2$	= position vectors of the centers of the two blocks connected with the block-connecting spring i
\mathbf{r}_j	= position vector of the center of the block connected with the anchoring spring j

$\mathbf{r}_{j,0}$ = anchoring position of the anchoring spring j
 $\mathbf{r}_Q(t)$ = position vector of the current path of output point Q at time t
 $\hat{\mathbf{r}}_Q(t)$ = position vector of the target path of output point Q at time t
 $\mathbf{s}_i^1, \mathbf{s}_i^2$ = position vectors from the centers of the two connected blocks to the block-connecting spring i
 \mathbf{s}_j = position vector from the center of the connected block to the anchoring spring j
 w = weight parameter for multi-objective formulation
 ϕ_A = input rotation angle
 ϕ_i = rotation angle of block i
 ξ_i = i th design variable

References

- [1] Kim, Y. Y., Jang, G. W., Park, J. H., Hyun, J. S., and Nam, S. J., 2007, "Automatic Synthesis of a Planar Linkage Mechanism With Revolute Joints by Using Spring-Connected Rigid Block Models," *ASME J. Mech. Des.*, **129**, pp. 930–940.
- [2] Bendsøe, M. P., and Sigmund, O., 1999, "Material Interpolation Schemes in Topology Optimization," *Arch. Appl. Mech.*, **69**, pp. 635–654.
- [3] Yoon, G. H., and Kim, Y. Y., 2003, "The Role of S-Shape Mapping Functions in the SIMP Approach for Topology Optimization," *J. Mech. Sci. Tech.*, **17**(10), pp. 1496–1506.
- [4] Chiou, S. J., and Kota, S., 1999, "Automated Conceptual Design of Mechanisms," *Mech. Mach. Theory*, **34**, pp. 467–495.
- [5] Lipson, H., and Pollack, J. B., 2000, "Automatic Design and Manufacture of Robotic Lifeforms," *Nature (London)*, **406**, pp. 974–978.
- [6] Pollack, J. B., and Lipson, H., 2000, "The GOLEM Project: Evolving Hardware Bodies and Brains," *Proceedings of the Second NASA/DoD Workshop on Evolvable Hardware*, July 13–15, Palo Alto, CA, pp. 37–42.
- [7] Fernández-Bustos, I., Aguirrebeitia, J., Avilés, R., and Angulo, C., 2005, "Kinematical Synthesis of 1-DOF Mechanisms Using Finite Elements and Genetic Algorithms," *Finite Elem. Anal. Design*, **41**, pp. 1441–1463.
- [8] Sedlacek, K., Gaugel, T., and Eberhard, P., 2005, "Topology Optimization Synthesis of Planar Kinematics Rigid Body Mechanism," *Multibody Dynamics, ECCOMAS Thematic Conference*, Madrid, Spain, June 21–24.
- [9] Kawamoto, A., Bendsøe, M. P., and Sigmund, O., 2004, "Articulated Mechanism Design With a Degree of Freedom Constraint," *Int. J. Numer. Methods Eng.*, **61**, pp. 1520–1545.
- [10] Ohsaki, M., and Nishiaki, S., 2007, "Generation of Link Mechanism by Shape-Topology Optimization of Trusses Considering Geometrical Non-linearity," *7th World Congress on Structural and Multidisciplinary Optimization*, COEX Seoul, Korea, pp. 1834–1841.
- [11] Tao, D. C., 1964, *Applied Linkage Synthesis*, Addison-Wesley Publishing Company, London.
- [12] Erdman, A. G., Sandor, G. N., and Kota, S., 1991, *Mechanism Design: Analysis and Synthesis Volume 1*, 2nd ed., Prentice-Hall, Inc., Englewood Cliffs, NJ.
- [13] Fox, R. L., and Gupta, K. C., 1973, "Optimization Technology as Applied to Mechanism," *ASME Trans. J. Eng. Ind.*, **95**, pp. 657–663.
- [14] Roots, R. R., and Ragesdell, K. M., 1976, "A Survey of Optimization Methods Applied to the Design of Mechanisms," *ASME Trans. J. Eng. Ind.*, **98**(3), pp. 1036–1041.
- [15] Howell, L., 2001, *Compliant Mechanisms*, John Wiley, New York.
- [16] Kimball, C., and Tsai, L. W., 2002, "Modeling of Flexural Beams Subject to Arbitrary End Loads," *ASME J. Mech. Des.*, **124**, pp. 223–235.
- [17] Jensen, B. D., and Howell, L. L., 2004, "Bistable Configuration of Compliant Mechanisms Modeled Using Four Links and Translational Joints," *ASME J. Mech. Des.*, **126**, p. 657.
- [18] Su, H. J., and McCarthy, J. M., 2007, "Synthesis of Bistable Compliant Four-Bar Mechanisms Using Polynomial Homotopy," *ASME J. Mech. Des.*, **129**, p. 1094.
- [19] Pedersen, C. B. W., Buhl, T., and Sigmund, O., 2001, "Topology Synthesis of Large-Displacement Compliant Mechanisms," *Int. J. Numer. Mech. Eng.*, **50**, pp. 2683–2705.
- [20] Sigmund, O., 1997, "On the Design of Compliant Mechanisms Using Topology Optimization," *Mech. Struct. Mach.*, **25**(4), pp. 493–524.
- [21] Kikuchi, N., Nishiaki, S., Fonseca, J. S. O., and Silva, E. C. N., 1998, "Design Optimization Method for Compliant Mechanisms and Material Microstructure," *Comput. Methods Appl. Mech. Eng.*, **151**, pp. 401–417.
- [22] Svanberg, K., 1987, "The Method of Moving Asymptotes a New Method for Structural Optimization," *Int. J. Numer. Mech. Eng.*, **24**, pp. 359–373.